BULLETIN OF THE EARTHQUAKE
RESEARCH INSTITUTE
Vol. 39 (1961). pp. 327-349

# 10. *Crustal Structure in Central Japan as Derived from the Miboro Explosion-Seismic Observations.*

## *Part 2. On the Crustal Structure.*

By Takeshi MIKUMO*, Michio ÔTSUKA**, Tokuji UTSU***, Tsutomu TERASHIMA**** and Atusi OKADA.*****

(Read Jan. 24, 1961.—Received June 30, 1961).

## 1. Introduction

This is one of a series of papers under the same title[1].

Crustal structure in central Japan, over the Kwantô, Tyûbu, Kinki and Tyûgoku Districts, will be discussed in some detail, making use of the data obtained by our group.

Detailed investigation of the underground structure by the refraction method generally requires repeated observations of seismic waves from two blasts at both sides of the profile along which observation stations are closely spread. Seismic waves from the Miboro Explosions were observed at the stations spreading along the Eastern and Western profiles, but no corresponding blast at the other end has yet been fired. The data obtained were one-sided.

Under these circumstances two standpoints may be possible in the way of analysis. One is as follows; some of unknown factors, such as propagation velocities in the crustal layers and the layer's thickness, will be assumed from previous knowledge based on past observational data, and then observed travel times will be interpreted so as to be consistent with these assumptions. The other is that; the apparent velocities of wave groups obtained from time-distance curves will be assumed to approximate the true ones in the respective crustal layers bounded by refracting horizons. The structure derived the from former standpoint is named by us Model I and the one from the latter Model II.

* Disaster Prevention Research Institute, the University of Kyôto.
** Geophysical Institute, Faculty of Science, the University of Kyôto.
*** Japan Meteorological Agency.
**** Geophysical Institute, Faculty of Science, the University of Tokyo.
***** Earthquake Research Institute, the University of Tokyo.

1) The Research Group for Explosion Seismology, *Bull. Earthq. Res. Inst.*, **39** (1961), 279-319.

Two of the probable models of crustal structure in each of the said profiles will be given. In the following analysis, travel times of the first compressional arrivals observed at the mentioned stations are mainly used with some reference to the later phases including S waves.

## 2. Travel Times near the Shot Point

As described in Part 1 of this paper, in the vicinity of the shot point at Miboro, pick-ups were set up along the left bank of Hukusima-valley, a quarrying site. The observed data at a total of 16 points in the I–VI explosions, except the No. II blast, are shown in Table 17 and Fig. 8 in the previous report. Looking at these results, analysis from the raw data seems to be difficult, owing to complicated factors, such as a certain extent of the shot area, the shooting procedure and topographical effects of the shot point and its environs.

An attempt will therefore be made here to reexamine the data, taking these effects into consideration.

1. On the shot time

The shot mark was registered through a lead-in wire connected

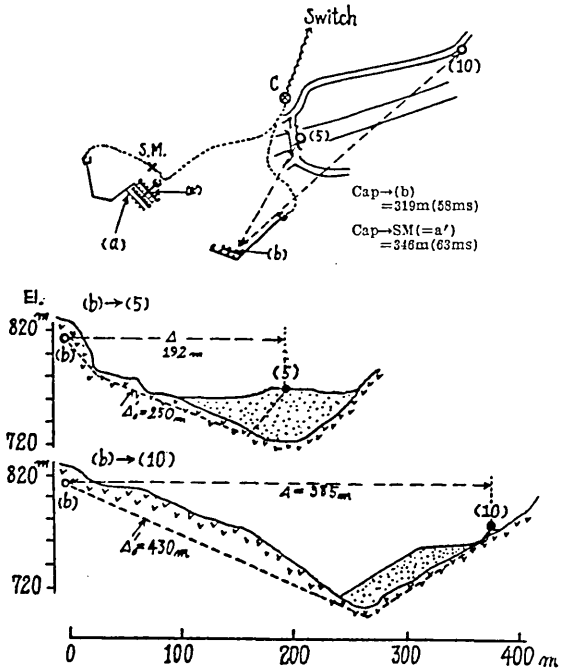


Fig. 1. An example of the explosion system and its profile.

with the point adjacent to an electrical blasting cap at the junction of detonating fuses leading to dynamite chambers or tunnels, except in the case of the No. VI explosion. Hence, the registered shot time should be corrected, taking the time delay into account, which elapsed in the detonating fuse between the cap and the nearest chamber. The delay is caused by the finite speed of firing. The value of 5.5 km/sec provided in JIS is adopted here as the detonation velocity in the prima chord. Using this value, the ignition time ($O'$) in the earlist detonated chamber can be deduced from the registered shot time ($O$) for each of the explosions.

2. On $\Delta$

The distance ($\Delta_0$) between the earliest ignited chamber and the pick-up does not coincide in general with the distance on plane ($\Delta$) between the nearest chamber and the pick-up. In the profile along a steep valley, the results may be much influenced by elevations and topography. For the present case the virtual distance ($\Delta_0'$) along the wave path between the nearest shot point and the pick-up was determined graphically for each of the profiles on a topographical map of 1/2000 precision. Fig. 1 shows a example of the profiles in the No. IV explosion.

3. Travel time analysis

Table 1. Reduced travel times near the shot point.

| No. | Obs. No. | P.U. No. | $\Delta$ | $\Delta_0'$ | (Corr.) | $P-O$ | $P-O'$ | (Corr.) |
|---|---|---|---|---|---|---|---|---|
| 1 | I | 1 | 39$^{m}$ | 50$^{m}$ | +11$^{m}$ | 24$^{ms}$ | 30$^{ms}$ | + 6$^{ms}$ |
| 2 | V | 1 | 114 | 118 | + 4 | 32 | 30 | − 2 |
| 3 | III | 1 | 124 | 173 | +49 | 93 | 74 | −19 |
| 4 | VI | 1 | 170 | 170 | 0 | 49 | 45 | − 4 |
| 5 | IV | 1 | 192 | 250 | +68 | 106 | 101 | − 5 |
| 6 | I | 2 | 225 | 260 | +35 | 102 | 108 | + 6 |
| 7 | III | 2 | 277 | 343 | +67 | 110 | 91 | −19 |
| 8 | V | 2 | 334 | 338 | + 4 | 84 | 82 | − 2 |
| 9 | VI | 2 | 373 | 375 | + 2 | 93 | 89 | − 4 |
| 10 | IV | 2 | 385 | 430 | +45 | 109 | 104 | − 5 |
| 11 | V | 3 | 483 | 490 | + 7 | 116 | 114 | − 2 |
| 12 | VI | 3 | 487 | 489 | + 2 | 114 | 110 | − 4 |
| 13 | III | 3 | 526 | 590 | +64 | 149 | 130 | −19 |
| 14 | IV | 3 | 575 | 623 | +48 | 146 | 141 | − 5 |
| 15 | VI | 4 | 646 | 652 | + 6 | 146 | 142 | − 4 |
| 16 | VI | 5 | 755 | 777 | +22 | 169 | 165 | − 4 |

The corrected results of the travel time and the distance, after the above stated procedure, $P-O'$ and $\Delta'$ are collectively listed in Table 1. In this treatment, the relative difference between the speed of waves from the nearest dynamite chamber and that from the earliest ignited one was examined from each observation point. The travel times shown in Table 1 are plotted versus distance in Fig. 2. Except for the data obtained at 6 points within a distance of 250 m, the relation between the travel times and the distances is given by the following formula, determined by the method of least squares.

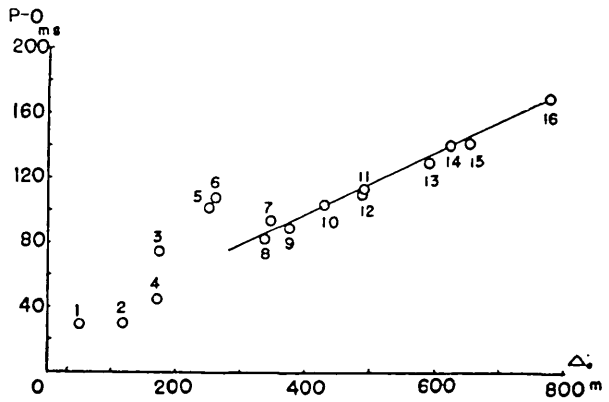


Fig. 2. Reduced travel time curves near the shot point.

$$T=\Delta_0'/5.53+0.025 \qquad \text{for pick-ups No. 7–16 in } 250<\Delta<760 \text{ m}.$$

The velocity of compressional waves in the said range is about 5.5 km/sec. It seems difficult to find a reasonable explanation for the scattering of the plots for $\Delta_0'<250$ m, but this may probably be attributed to the effects of the irregular weathered layer on which the pick-ups were set.

## 3. Crustal Structure in the Tyûbu and Kwantô Districts (the Eastern Profile)

### § 1. Time-Distance Curves

The reduced time-distance graph in the Eastern profile is shown in Fig. 3, by the use of the data tabulated in Table 14 in Part 1 of this paper. In this figure $P-O-\Delta/6$ is taken as the ordinate to study detailed features of the travel times.

There may be some ways of drawing reasonable curves, but two

cases are adopted here from the representative standpoints mentioned before.

The travel times fitted to each of the branches are represented as the following formulae for Models I and II.

M–I
$$\begin{cases} P_1\ ;\ T_1=\Delta/5.55+0.16 & \text{for Myôgase-Kotakari} & (\quad \Delta< 28\text{ km}) \\ P_{21}\ ;\ T_{21}=\Delta/5.86+0.43 & \text{for Kamioka-Matusiro} & (28<\Delta<130\text{ km}) \\ P_{22}\ ;\ T_{22}=\Delta/6.33+2.07 & \text{for Matusiro-Ôiwa} & (130<\Delta<175\text{ km}) \\ P_3\ ;\ T_3=\Delta/7.91+8.18 & \text{for Takayama-Nisioasi} & (185<\Delta\quad \text{km}) \end{cases}$$

M–II
$$\begin{cases} P_1\ ;\ T_1=\Delta/5.55+0.16 & \text{for Myôgase-Kotakari} & (\quad \Delta< 38\text{ km}) \\ P_2\ ;\ T_2=\Delta/6.00+0.68 & \text{for Kamioka-Ôiwa} & (38<\Delta<185\text{ km}) \\ P_3\ ;\ T_3=\Delta/7.90+8.13 & \text{for Takayama-Nisioasi} & (185<\Delta\quad \text{km}) \end{cases}$$

Analysis will be made solely by using the travel time equations[2].

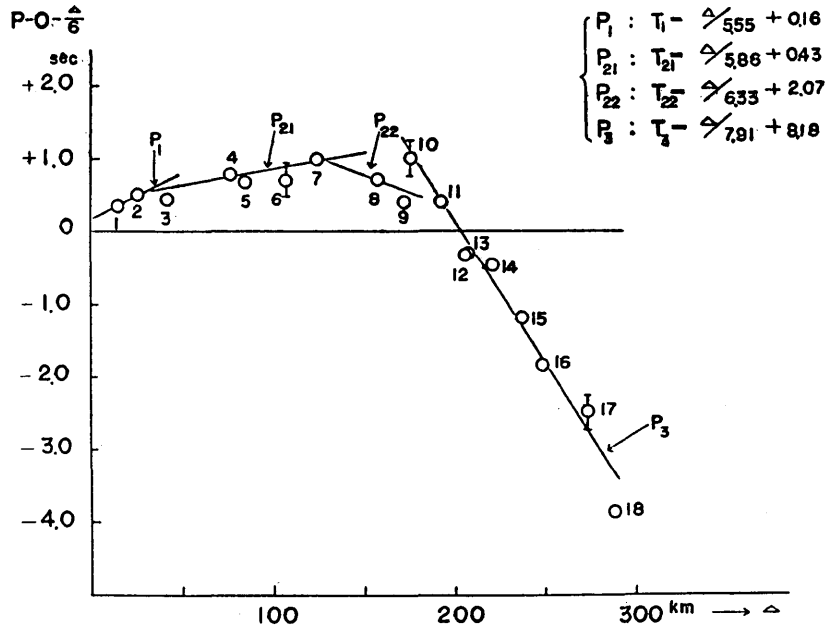


Fig. 3. Reduced travel time curves in the Eastern profile.

## § 2. Model I

### 1. Travel times of $P_1$ and the superficial layer

The apparent velocity of $P_1$ waves, 5.55 km/sec, is adopted as the true velocity in the 1st layer. This value agrees well with the corresponding velocity in the Western profile, the data from observation

2) Report R. G. E. S., (1961), in preparation.

near the shot point and the result obtained in the Kwantô District[3].

The intercept time of $P_1$, 0.16 sec, suggests the possible existence of a superficial layer with a lower velocity overlying the 1st layer. Near the shot point, however, the velocity of 5.53 km/sec corresponding to that in the 1st layer is observed beyond a distance of 250 m. On the contrary, the intercept time is nearly zero in the case of the Western profiles. These facts indicate that the weathered layer may be negligibly thin beneath the shot point at Miboro. The superficial layer with unknown low velocity is assumed to exist only near Myôgase and Kotakari stations.

2. Travel times of $P_2$ and the thickness of the first layer

The true velocity of longitudinal waves in the 2nd layer is assumed to be 6.00 km/sec, from the results of explosion observation in the Kwantô District. Two branches of the $P_2$ waves suggest a downwarping of the layer.

(1) The interface between the 1st and 2nd layers is estimated to descend eastwards with a dip of 3.4° through the apparent velocity of $P_{21}$ waves, 5.86 km/sec. The intercept time 0.43 sec of $P_{21}$ indicates the boundary depth of 3.1 km, that is, 2.3 km below sea level. To conform, however, with the data from the Western profiles, the first layer is assumed to taper to a thickness of 1.8 km from $\Delta=10$ km to the shot point.

(2) The apparent velocity 6.32 km/sec of $P_{22}$ waves indicates that the above interface changes its inclination and begins to ascend eastwards with a dip of 6.2°. The deepest point is at $\Delta=115$ km with a depth of 9.2 km, which is computed from the intercept time 2.07 sec of $P_{22}$ and the velocities in the two layers. The corresponding depth at $\Delta=152$ km is 5.0 km.

The arrival of $P_{22}$ waves observed at Ôiwa is so earlier than to be expected from calculated travel time for the deduced structure. This may be attributed to the fact that the 2nd layer crops out to the earth's surface between Hoppo and Ôiwa. This is confirmed also by the results of Kwantô explosions.

(3) As for the thickness of the 1st layer with the velocity of 5.55 km/sec beyond Takayama station, the value of 6 km is adopted so as to be consistent with the explosion data in the Kwantô region.

3. Travel times of $P_3$ and the thickness of the second layer

The true velocity in the 3rd layer is assumed to be 7.70 km/sec in

3) T. USAMI *et al.*, *Bull. Earthq. Res. Inst.*, **36** (1958), 349-357.

accordance with the observational data from the Kwantô District. The discontinuity surface between the 2nd and 3rd layers is considered to ascend eastwards with a dip of 1.8°, in view of the apparent velocity 7.91 km/sec of $P_3$ waves. A tentative estimation gives a round value of 38 km for the boundary depth beneath Miboro. From the data for the Western profiles, however, the depth in various probable models is estimated to be 27–29 km under any assumption. On the other hand, the boundary has already been found to be about 25–30 km in the Kwantô region. These data suggest a downward warping of the 2nd layer. That is, the discontinuity surface along the said profile is supposed to descend eastwards from Miboro and in turn begin to ascend toward the Kwantô area. The ray paths of the mentioned waves in this profile are schematically represented in Fig. 4.

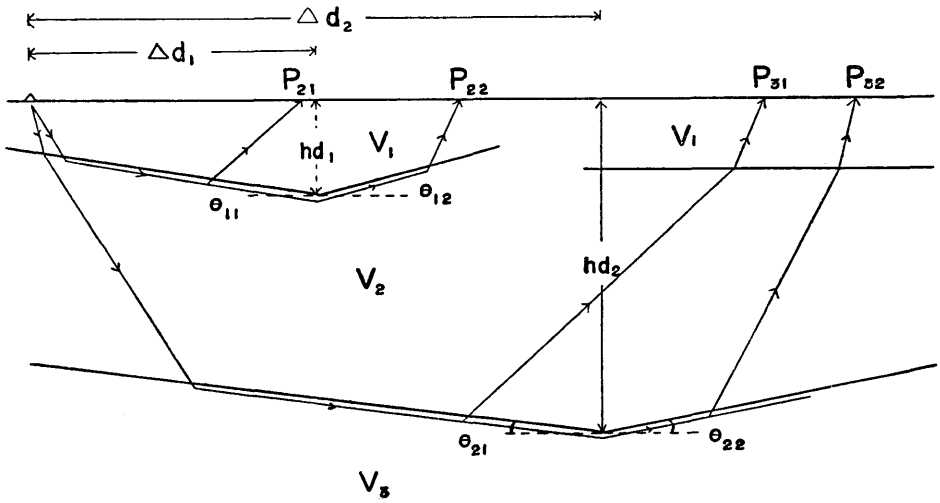


Fig. 4. Schematic representation of ray paths in Model I.

(1) The diffracted waves $P_{32}$ are to arrive as first waves beyond Takayama. The ascending inclination $\theta_{22}$ of the discontinuity is 1.8° as determined above. The boundary depth beneath Miboro is assumed to be 27.7 km below sea level, so as to be consistent with the Western profile data.

(2) Concerning a descending dip $\theta_{21}$, no direct evidence is found. For this reason, therefore, a possible limit of $\theta_{21}$ is estimated only from the following simultaneous conditions.

One is a geometric condition that the $P_{32}$ waves emerge first beyond Takayama. The other is the condition keeping the intercept time of

$P_{32}$ 8.18 sec. The limit is determined as $\theta_{21} \geqq 3.9°$. The value of 4.0° is adopted in the present case with a view to minimizing the inclination.

(3) Using the intercept time and the velocities in the respective layers, the deepest boundary is found to occur at $\Delta = 149$ km, and its depth is 38.1 km. The depth at a distance of 250 km is 35.0 km.

(4) The arrivals of $P_3$ waves observed at Huziwara, Kawaba and Tukuba are earlier than to be expected from calculation of this model. These are attributable to outcrop of the 2nd layer near the stations. The anomalous delay at Asakawa indicates the possible existence of material characterized by a low velocity at the surface. Along a profile including Miboro and Tukuba, the interface between the 2nd and 3rd layers is believed to ascend from the deepest point with a dip of 3.9°, and to have a value of 28.0 km beneath Tukuba. The crustal structure in the vicinity of the station accords with that determined by the results in the Kwantô District.

## § 3. Model II

The apparent velocities, 5.5, 6.0 and 7.9 km/sec, of the $P_1$, $P_2$, and $P_3$ waves traveling through the 1st, 2nd and 3rd layers are assumed to be the substantial values of longitudinal waves in the respective layers bounded by horizontal velocity discontinuities.

1. Superficial layer

This is assumed to be the same as in the case of Model I.

2. 1st layer

Calculating from the intercept time of $P_2$, 0.68 sec, together with the velocities in the 1st and 2nd layers, the former is estimated two to be about 5 km thick, that is, the boundary depth between the above two to be 4.2 km below sea level.

The early arrivals of $P_2$ waves observed at Kamioka and Ôiwa would be indicative of exposure of the 2nd layer to the surface near the stations. A possible explanation of the late arrival at Matusiro is a local velocity irregularity. As for the thickness of the 1st layer at a great distance, the already determined value of 6 km in the Kwantô region is adopted here.

3. 2nd layer and 3rd layer

The $P_3$ waves emerge as initial arrivals beyond the distance of Takayama. The intercept time 8.13 sec of $P_3$, the afore-mentioned 1st layer's thickness and the velocities indicate that the depth of the interface between the 2nd and 3rd layers is 35.6 km beneath sea level.

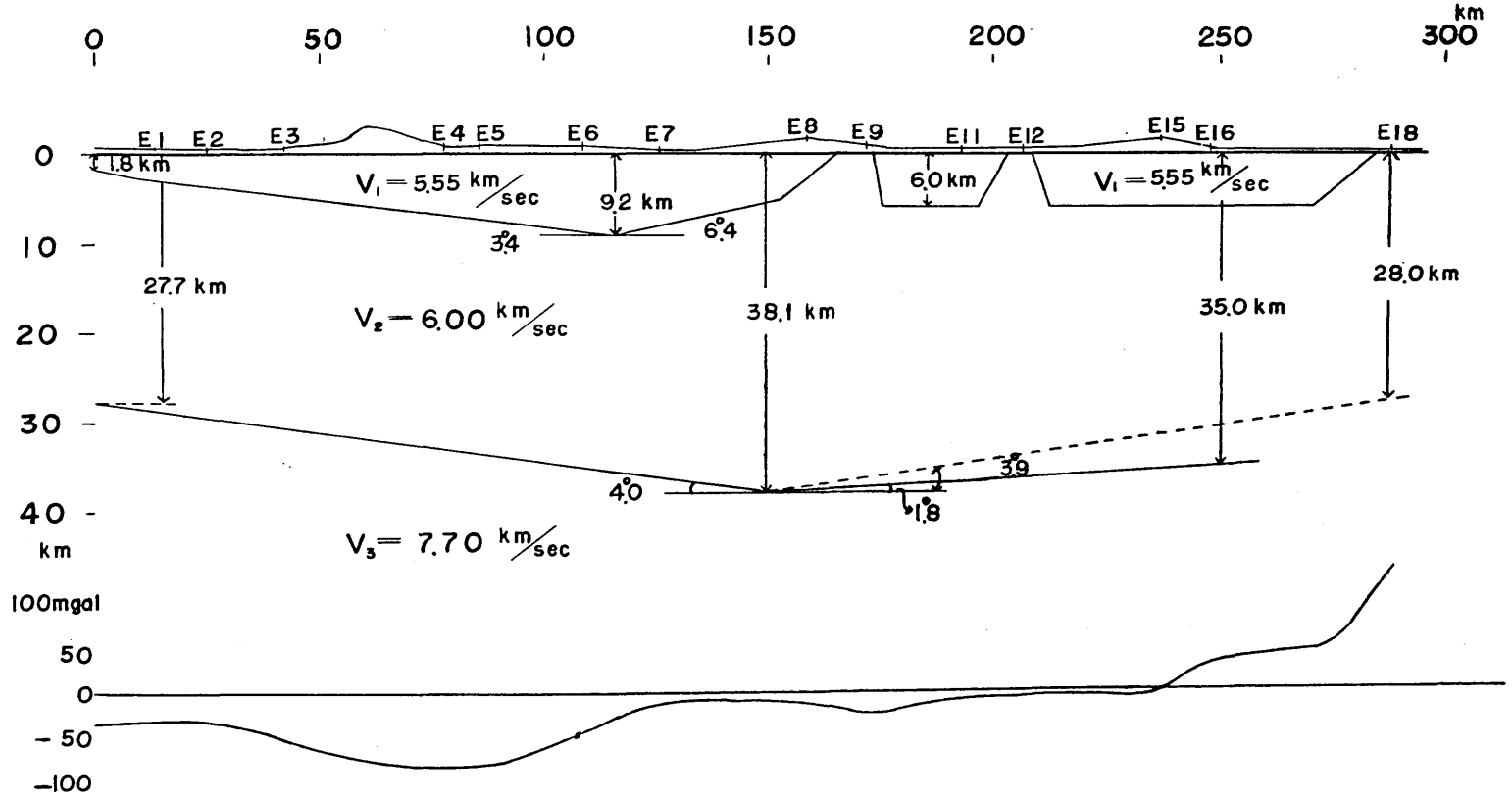


Fig. 5(a). Crustal structure in the Eastern profile. Model I, with Bouguer anomaly of gravity along the profile.

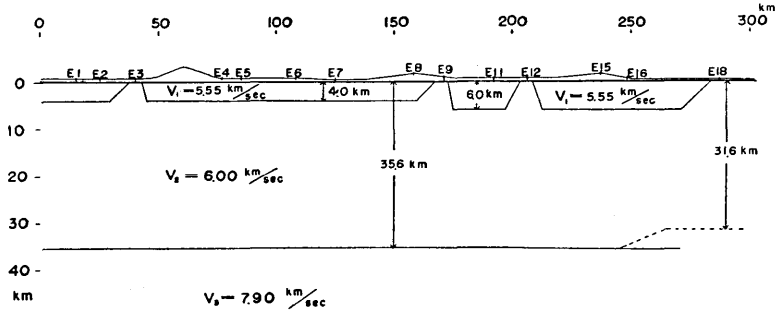


Fig. 5(b). Crustal structure in the Eastern profile. Model II.

The early arrivals observed at Huziwara, Kawaba and Tukuba are believed to result partly from the upheaval of the 2nd layer. If the discontinuity between the 2nd and 3rd layers becomes shallower by 4 km from $\Delta=250$ km, the short travel time at the last station is satisfactorily interpreted. The observed delay at Asakawa is attributed to a low velocity weathered layer.

## § 4. Results and Discussion

### 1. The derived structure and the travel time residuals

Two models of the crustal structure derived from the foregoing analysis are presented in Figs. 5 (a) and 5 (b). The boundary depth is indicated by the value below sea level. The travel times to each station calculated for the deduced structure are tabulated in Table 2. In this

Table 2. Calculated travel times and $O-C$ residuals for each station in the Eastern profile.

| | Station | $T_0$ (sec) | Model I $T_c$ (sec) | Model I $T_0-T_c$ (sec) | Model II $T_c$ (sec) | Model II $T_0-T_c$ (sec) |
|---|---|---|---|---|---|---|
| E 1 | Myôgase | 2.91 | $P_1$ 2.75 | 0.16 | $P_1$ 2.75 | 0.16 |
| 2 | Kotakari | 4.82 | 〃 4.67 | 0.15 | 〃 4.67 | 0.16 |
| 3 | Kamioka | 7.37 | $P_{21}$ 7.52 | −0.14 | $P_2$ 7.43* | −0.06 |
| 4 | Inekoki | 13.66 | 〃 13.62 | 0.04 | 〃 13.56 | 0.10 |
| 5 | Hotaka | 14.85 | 〃 14.98 | −0.13 | 〃 14.90 | −0.05 |
| 6 | Omi | 18.8 | 〃 18.96 | −0.2 | 〃 18.79 | 0.0 |
| 7 | Matusiro | 21.87 | 〃 21.82 | 0.06 | 〃 21.55 | 0.32 |
| 8 | Hoppo | 27.22 | $P_{22}$ 27.19 | 0.03 | 〃 27.18 | 0.04 |
| 9 | Ôiwa | 29.01 | 〃 29.00* | 0.01 | 〃 29.13* | −0.12 |
| 10 | Sawatari | 30.4 | (L) $P_{31}$ 30.48 | −0.1 | (L) $P_3$ 30.45 | −0.1 |
| 11 | Takayama | 32.58 | $P_{32}$ 32.59 | −0.01 | $P_3$ 32.58 | 0.00 |
| 12 | Huziwara | 33.98 | 〃 34.10* | −0.12 | 〃 34.09* | −0.11 |
| 13 | Kawaba | 34.09 | 〃 34.13* | −0.04 | 〃 34.13* | −0.04 |
| 14 | Asakawa | 36.33 | 〃 36.06 | 0.27 | 〃 36.04 | 0.29 |
| 15 | Yumoto | 38.38 | 〃 38.33 | 0.05 | 〃 38.31 | 0.07 |
| 16 | Nisioasi | 39.61 | 〃 39.60 | 0.01 | 〃 39.59 | 0.02 |
| 17 | Sinoi | 43.2 ? | 〃 42.80 | (0.4) | 〃 42.79 | (0.4) |
| 18 | Tukuba | 44.17 | 〃 44.17* | 0.00 | 〃 44.17* | 0.00 |

Remarks: 1) (L); later phase
2) * ; The second layer crops out to the earth's surface.
3) $T_0$; observed travel time, $T_c$; calculated travel time.

calculation, corrections are made for the height difference between the shot and the observation point.

The difference between the observed and calculated travel times, which is called $O-C$ residual by our group, is reconciled within 0.15 sec except for the ones at Myôgase, Kotakari and Asakawa, in Model I. An exception is further added for Matusiro to Model II. All of these deviations may be responsible for a weathered layer.

2. Remarks on the observation of reflected waves

In the third observation, prominent later phases were recorded on the seismogram at Kamioka station where additional study of the seismic reflection method was attempted[4].

With a view to identifying reflected phases in the seismogram, travel times of reflections are computed concerning the derived structure. That of the waves reflected from the interface between the 1st and 2nd layers is 7.46 sec in Model I and 7.68 sec in Model II, but no corresponding phase was observed. As to the reflection from the boundary between the 2nd and 3rd strata, it takes 12.20 sec in Model I and 13.87 sec in Model II. The former time agrees well with the observed one of 12.21 sec. There is a little doubt, however, in concluding that this is related to the waves reflected from the Mohorovičić discontinuity, because the observed apparent velocity of 6.86 km/sec is smaller than the expected value of 9.35 km/sec. Judging from the recorded wave forms and observed apparent velocity, the phase with a travel time of 12.72 sec and a velocity of 11.38 km/sec seems to be the reflected waves from the said discontinuity. If this is true, the boundary should be corrected as being shallower by 1.3 km.

3. Remarks on the Bouguer anomaly of gravity

The Bouguer anomaly of gravity[5] distributed along the present profile indicates a great negative value in the Tyûbu mountain region, as shown in Fig. 5 (a). It may roughly be said that the downward warping of the 1st and 2nd layers near the region corresponds to this great negative anomaly. Morever, an increasing positive anomaly toward Tukuba may probably be caused by a localized upheaval of the 2nd and 3rd layers. The derived structure is not inconsistent with the gravity data.

4) S. MURAUCHI, *Report R. G. E. S.*, No. 17 (1958), 9-10.

5) C. TSUBOI *et al.*, *Bull. Earthq. Res. Inst., Suppl.* **4** (1955), Part 5; (1956), Part 7.

## 4. Crustal Structure in the Tyûbu, Kinki and Tyûgoku Districts (the Western profile)

### § 1. Time-Distance Curves

Reduced travel times in the Western profiles are plotted in Figs. 6 and 7, by the use of the data listed in Tables 15 and 16 in Part 1 of this paper.

The travel times of each wave group are represented as the following formulae for Models I and II in two Western profile. Profile A designates the northern section including the Hokuriku—northern Kinki—Tyûgoku regions and Profile B indicates the southern section traversing the central part of the Kinki District.

1. Profile A

| | | | | |
|---|---|---|---|---|
| M–I | $P_{21}$; | $T_{21}=\Delta/5.92+0.31$ | for Nakai-Mikata | ( $28<\Delta<102$ km) |
| | $P_{22}$; | $T_{22}=\Delta/6.32+1.41$ | for Mikata-Yasiro | ($102<\Delta<165$ km) |
| | $P_3$; | $T_3=\Delta/7.52+5.98$ | for Hukutiyama-Yanahara | ($165<\Delta$ km) |
| M–II | $P_2$; | $T_2=\Delta/6.00+0.46$ | for Nakai-Ôi | ( $50<\Delta<160$ km) |
| | $P_3$; | $T_3=\Delta/7.50+5.82$ | for Yatuai-Yanahara | ($160<\Delta$ km) |

2. Profile B

| | | | | |
|---|---|---|---|---|
| M–I | $P_1$; | $T_1=\Delta/5.55$ | for Arabuti-Itosiro | ( $\Delta<28$ km) |
| | $P_{21}$; | $T_{21}=\Delta/5.81+0.31$ | for Ôgawara-Kitoge | ( $28<\Delta<112$ km) |
| | $P_{22}$; | $T_{22}=\Delta/6.16+1.40$ | for Sirahige–Sikibi. | ($112<\Delta<168$ km) |
| | $P_3$; | $T_3=\Delta/7.45+6.13$ | for Taki-Tainohata | ($168<\Delta$ km) |
| M–II | $P_1$; | $T_1=\Delta/5.50$ | for Arabuti-Ôno | ( $\Delta<45$ km) |
| | $P_2$; | $T_2=\Delta/6.00+0.46$ | for Ôgawara | |
| | $P_2'$; | $T_2'=\Delta/6.00+0.70$ | for Gihu-Kyoto | ( $70<\Delta<165$ km) |
| | $P_3$; | $T_3=\Delta/7.50+6.21$ | for Sikibi.-Kitaama | ($165<\Delta$ km) |

### § 2. Model I

#### 2–1. Profile A (Northern Section)

1. Travel times of $P_1$ and the superficial layer

As is the case in the Eastern profile, the apparent velocity of the $P_1$ waves, 5.55 km/sec, is adopted as the true one for the longitudinal waves in the 1st layer, common to both of the Profiles A and B. The superficial layer overlying the 1st one, near the shot point, can be omitted in the present case, considering that the intercept time of $P_1$ is negligibly small.

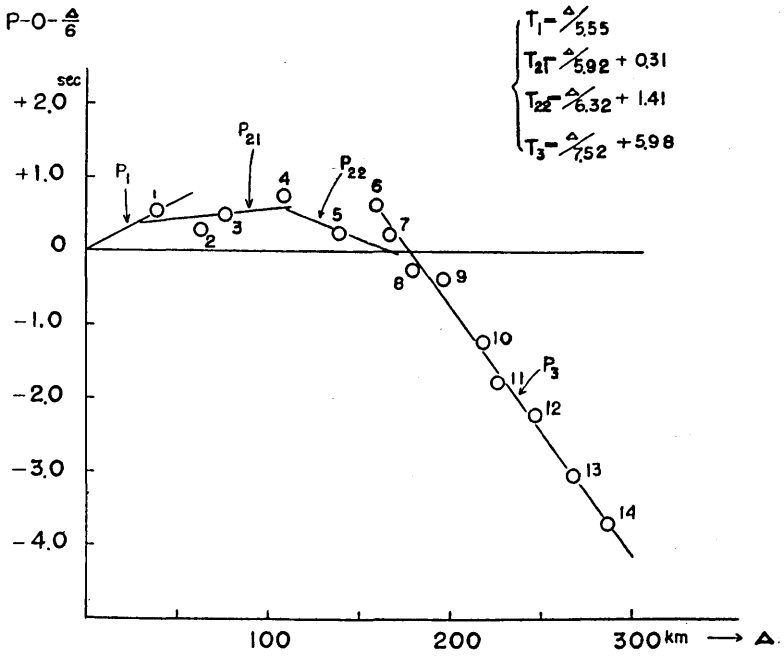


Fig. 6. Reduced travel time curves in the Western profile A.

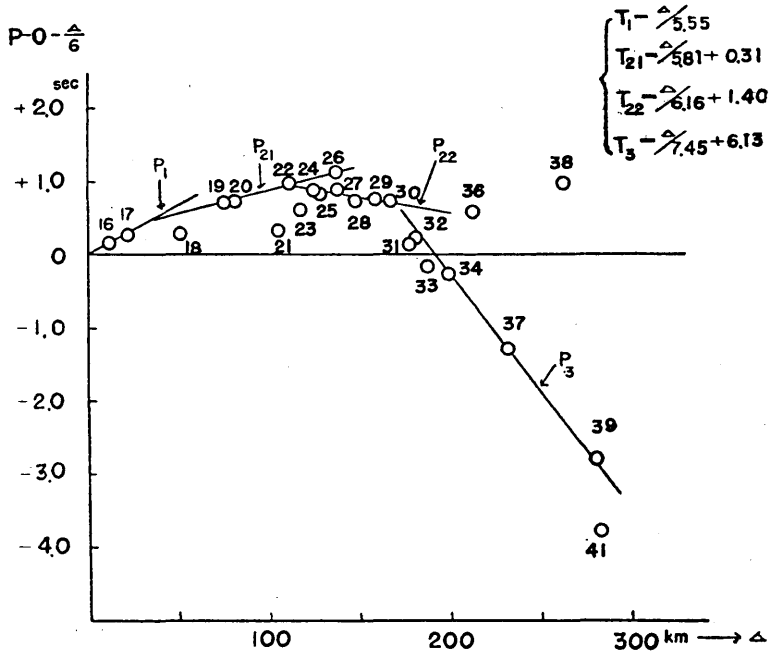


Fig. 7. Reduced travel time curves in the Western profile B.

2. Travel times of $P_2$ and the thickness of the first layer

The true velocity of the compressional waves in the 2nd layer is assumed to be 6.00 km/sec, in accordance with the adopted value in the Eastern profile.

(1) When calculated from the apparent velocity of the $P_{21}$ waves, 5.92 km/sec, the interface between the 1st and the 2nd layers is estimated to descend westwards with a dip of 2.0°. The thickness of the 1st layer beneath the shot point at Miboro is calculated as being about 2.6 km (that is, the depth of the interface is 1.8 km below sea level), from the intercept time of $P_{21}$, 0.31 sec.

The shorter travel time observed at Nakai is supposed to be due to the outcropping of the 2nd layer, lacking of the 1st one near the station.

(2) The apparent velocity of the $P_{22}$ waves is 6.32 km/sec. It can therefore be considered that the above-mentioned boundary begins to ascend westwards with a dip of 6.3°. Using the intercept time 1.41 sec of $P_{22}$ and the velocities in the two layers, the deepest point is found to occur at $\Delta$=96.4 km with a depth of 5.1 km. As the interface is exposed to the surface at $\Delta$=143 km, the 2nd layer is considered to crop out between Yasiro and Hukutiyama.

(3) The thickness of the 1st layer at a great distance will be determined from the travel times of $P_3$ waves.

3. Travel times of $P_3$ and thickness of the second layer

The true velocity of longitudinal waves in the 3rd layer is assumed to be 7.70 km/sec, so as to be consistent with the adopted value for Model I in the Eastern profile and the result obtained in the Kwantô District.

(1) The apparent velocity 7.52 km/sec of $P_3$ waves can be explained by a westerly-downward dip of 1.7° of the discontinuity surface between the 2nd and 3rd layers.

(2) The depth to the discontinuity cannot be determined only from the intercept time of $P_3$, without a knowledge of the thickness of the 1st layer at a great distance.

The $P_3$ waves are observed as initial arrivals beyond Hukutiyama. The early arrival of the waves at this station is assumed to be caused by the 2nd layer's outcrop to the surface. The travel time at Hukutiyama and the intercept time of $P_3$ offer information about the boundary depth between the 2nd and 3rd strata, under the condition that the thickness of the 1st layer beyond Aogaki retains reasonable value. This consideration leads to 27.7 km in the mean depth below sea level. The

corresponding depth at $\Delta=290$ km is 36.5 km.

(3) For the sake of simplicity, a horizontal interface is assumed between the 1st and 2nd layers beyond Aogaki station. From the travel times of $P_3$, the 1st layer's thickness is derived as being about 8.5 km at Aogaki, Ikuno and Yamazaki, and 2.5 km at Kamigôri and Yanahara. The early arrival observed at Kawakami may indicate the 2nd layer's exposure to the earth's surface.

### 2-2. Profile B (Southern Section)

As to the substantial velocities in the respective layers, the assumed values in the case of Profile A are adopted.

1. Travel times of $P_1$

These are common to the case of Profile A.

2. Travel times of $P_2$ and the thickness of the first layer

(1) The boundary between the 1st and 2nd layers is estimated to have a downward dip of 5.7°, from the data of the apparent velocity 5.81 km/sec of $P_{21}$ waves. The same value for the intercept time of $P_{21}$ as in Profile A gives nearly the same result for the 1st layer's thickness beneath the shot point, in spite of a slight difference in the dip angle. The shorter travel time observed at Ôgawara is attributable to the outcrop of the 2nd layer.

This model of the structure offers no satisfactory explanation as to the extremely early arrival of $P_{21}$ at Kaizu.

(2) The apparent velocity 6.16 km/sec of $P_{22}$ waves gives the boundary surface ascending westwards from the deepest point with a dip of 3.7°. The epicentral distance of the deepest point is calculated to be at $\Delta=86.8$ km with a depth of 9.5 km, from data of the intercept time 1.40 sec and the velocities in the two the layers. The depth of the interface is 5.3 km at $\Delta=160$ km.

(3) The thickness of the 1st layer at a great distance will be estimated from the travel times of $P_3$ waves. This is considered to be thicker than that in Profile A, on account of the larger intercept time.

3. Travel times of $P_3$ and the thickness of the second layer

(1) The discontinuity between the 2nd and 3rd strata is estimated to have a westerly-downward dip of 2.6°, from the apparent velocity of $P_3$, 7.45 km/sec. The depth to this boundary is calculated as 36.4 km at $\Delta=190$ km, being the same depth beneath the shot point as in the case of Profile A.

(2) The $P_3$ waves are observed as initial arrivals beyond Kameoka.

The intercept time of $P_3$, 6.13 sec indicates a thickness of 9.5 km for the 1st layer beyond Ôharano, under the assumption of a horizontal interface.

The earlier arrivals observed at Kameoka, Taki and Abuyama stations are believed to be the result of an outcrop of the 2nd layer to the surface. The observed times at Rokkô and Sizuki are interpreted to be those of the later phase $P_{2_2}$, judging from calculated results of the wave propagation.

(3) A possible explanation of the early arrival at Kitaama (Awazi Isl.) is that the discontinuity between the 2nd and 3rd strata ascends westwards with a dip of 6.8° from a distance of 194 km having a depth of 25.2 km below the station.

## § 3. Model II

The apparent compressional velocities, 5.5, 6.0 and 7.5 km/sec, of the $P_1$, $P_2$ and $P_3$ waves traveling through the 1st, 2nd and 3rd layers are assumed to be the true ones in the respective layers, common to both of the Profiles A and B.

As in the case of Model I, the superficial layer is neglected because of the zero intercept of $P_1$ waves.

### 3-1. Profile A (Northern Section)

1. 1st layer

The depth to the boundary between the 1st and 2nd layers is calculated as 3.2 km below the shot point, that is, 2.4 km below sea level, from the data of the intercept time of $P_2$ and the wave velocities.

The arrival times observed at Nakai and Ôi are earlier than those expected from the derived structure, and that at Mikata is later than the calculated times. To give a possible explanation to these deviations, it is considered that the 2nd layer crops out to the surface at Nakai with a tapering of the 1st layer from $\Delta=50$ km, that the 1st layer's thickness increases to 6 km from $\Delta=90$ km, and that it again tapers from $\Delta=105$ km with an outcrop of the 2nd layer at Ôi.

2. 2nd layer and 3rd layer

The longitudinal waves $P_3$ passing through the 3rd layer emerge as initial arrivals beyond Yatuai. From the standard equations of the travel times, the 2nd layer is found to be as thick as 25.2 km below the shot point, namely, the boundary depth between the 2nd and 3rd layers is 27.6 km.

The assumed thickness of 2.4 km for the 1st layer between Yatuai and Hukutiyama gives an earlier arrival in the calculation than the observed time for the former station. It is believed that the observed arrival is related to the later phase. The delayed arrivals observed at Aogaki, Ikuno and Yamazaki are considered to be attributable to increased thickness of the 1st layer to about 13 km.

Calculating from the observed travel times of $P_3$, the 1st layer's thickness is estimated to be 2.4 km below Kawakami and 6 km below Kamigôri and Yanahara stations.

### 3-2. Profile B (Southern Section)

1. 1st layer

The early arrival observed at Ôgawara may be the result of the 1st layer tapering from $\Delta=30$ km and the 2nd one cropping out to the surface near the station.

Beyond Gihu, the thickness of the 1st layer is estimated as 5.7 km from the intercept time of $P_2$, which is a little larger than the previously determined value at a short distance.

To interpret the observed early arrival at Kaizu, it is necessary to consider that the 2nd layer is exposed to the surface at the station with a tapering of the 1st layer from $\Delta=80$ km. If we approve of this point-of-view, however, we find it difficult to give a satisfactory explanation to the delayed arrivals observed at several points between Kitoge and Wani. The onset of the waves is not so clearly observed at all of these stations which are located along the west coast of Lake Biwa. For this reason, data from these stations are omitted in the present treatment. In order to adjust the calculated values to the observed ones for the said stations, we have to suppose the existence of the superficial layer with a lower velocity overlying the the 1st layer.

2. 2nd layer and 3rd layer

The phase $P_3$ traveling through the 3rd layer appears as an initial arrival beyond Sikibigahara. The 2nd layer's thickness is computed as 23.0 km and therefore the boundary depth as 28.7 km, using the intercept time of $P_3$.

The late arrivals observed at Ôharano and Tainohata are explained by the thickening of the 1st layer between $\Delta=180$ km and 250 km, being 15.3 km. The arrival time at Kitaama is anomalously early. It is impossible to interpret this fact only by the decrease in the 1st layer's thickness, so that the discontinuity between the 2nd and 3rd strata is

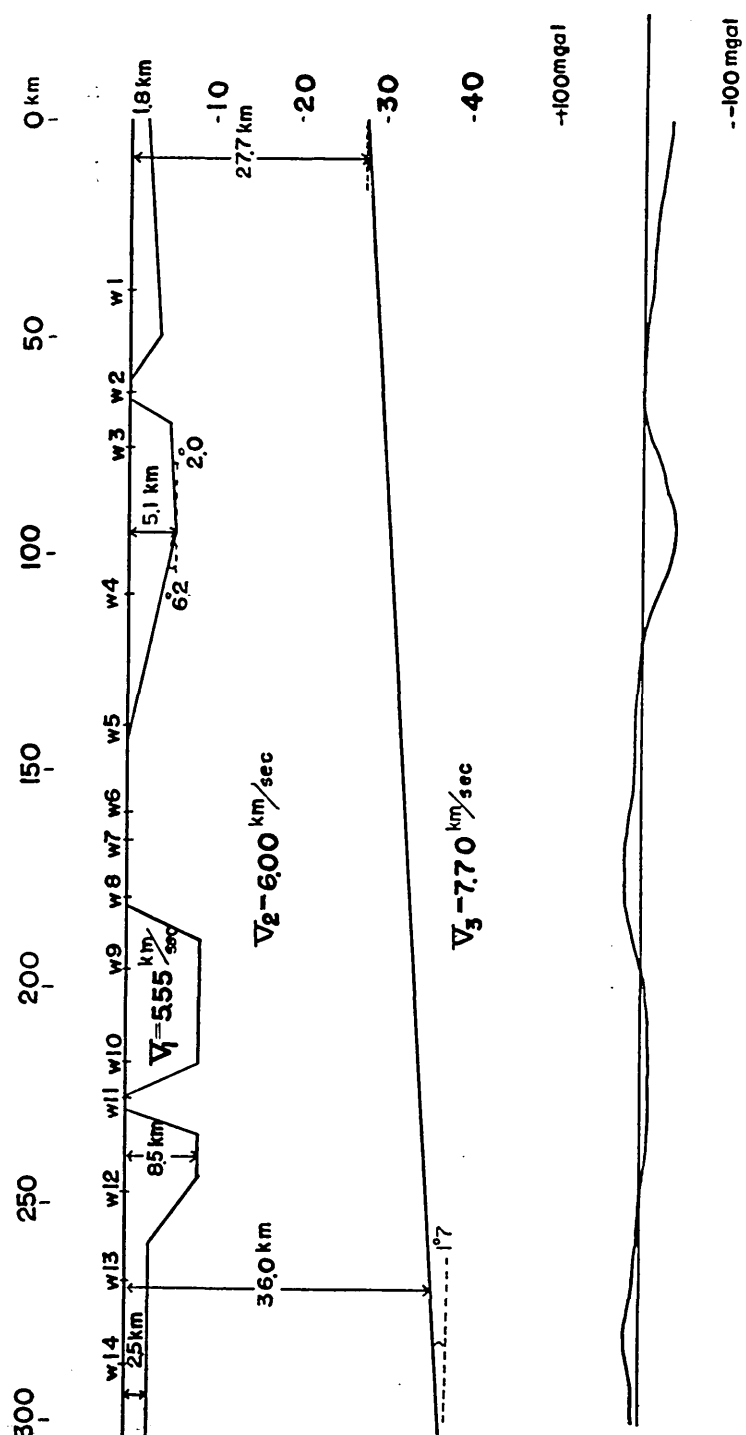


Fig. 8 (a). Crustal structure in the Western profile A. Model I, with Bouguer anomaly of gravity along the profile.

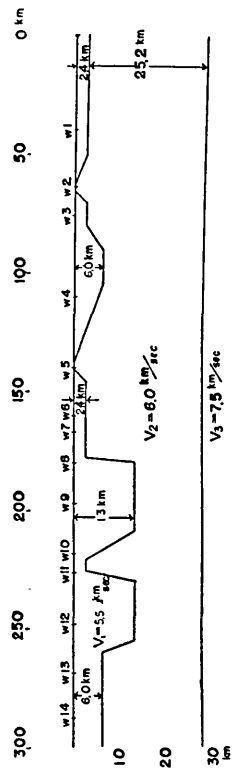


Fig. 8 (b). Crustal structure in the Western profile A. Model II.

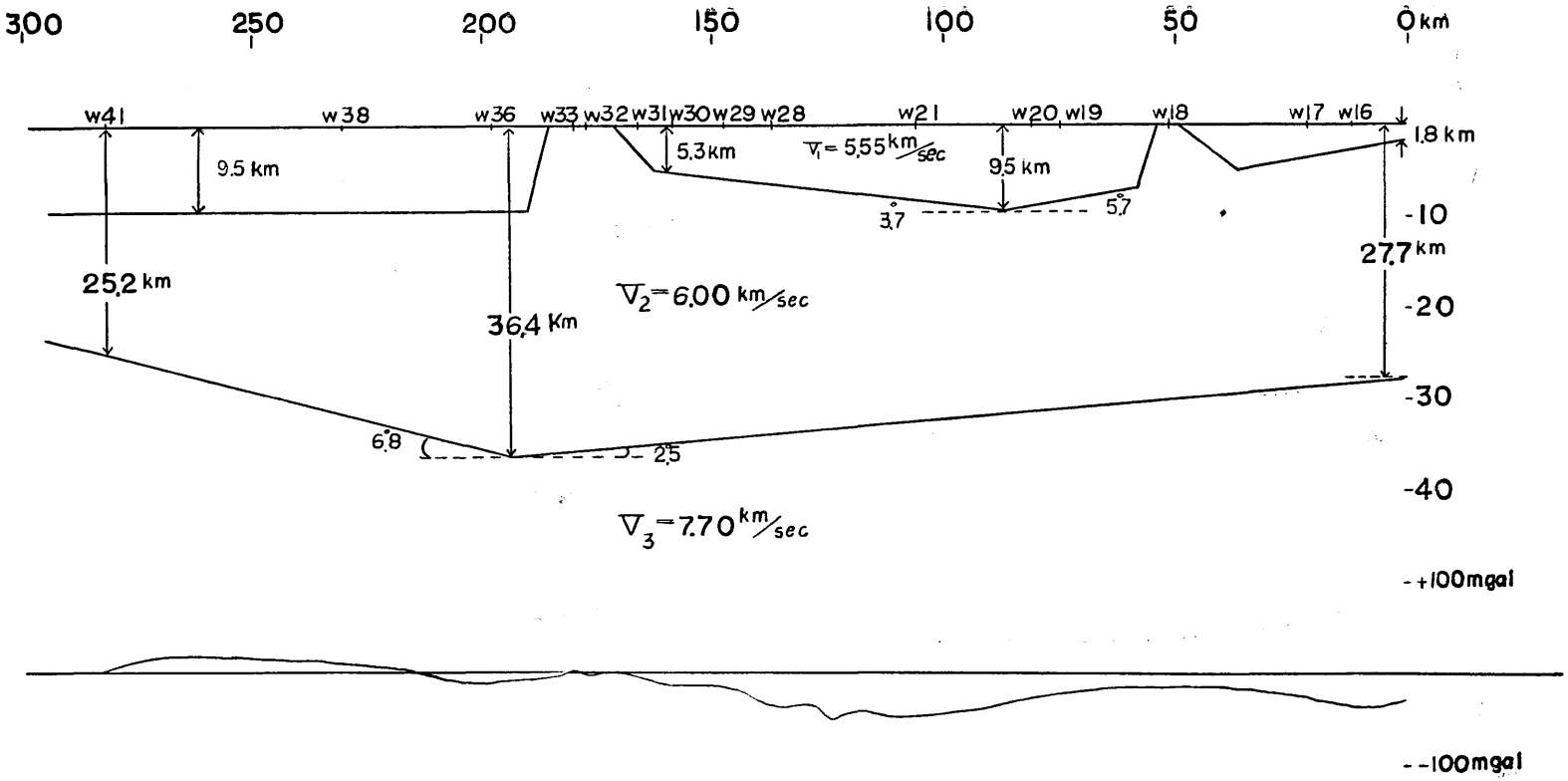


Fig. 9(a). Crustal structure in the Western profile B. Model I, with Bouguer anomaly of gravity along the profile.

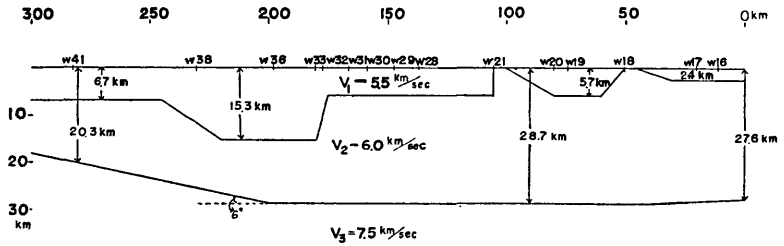


Fig. 9(b). Crustal structure in the Western profile B. Model II.

thought to dip upwards by 6° from $\Delta=200$ km.

The data obtained at Rokkô, Sizuki and Suhara were omitted in this analysis because of obscurity in their initial phases. The observed values at the former two stations are probably connected with those of a later phase.

## § 4. Results and Discussion

1. The derived structure and the travel time residuals

Two probable models of crustal structure derived from the foregoing analysis for both the Western profiles are presented in Figs. 8 (a), (b) and 9 (a), (b).

Tables 3 and 4 summarize the calculated travel times for the deduced models, together with $O-C$ residuals at each of the stations. Elevation corrections are made in these values.

$O-C$ residuals for Model I are within 0.15 sec except those at Mikata, Kaizu, Hukutiyama and at a few points where observational accuracy was not so good. For Model II, $O-C$ values are reconciled within 0.12 sec except for the ones at Aogaki and the 6 stations on the west coast of Lake Biwa.

Table 3. Calculated travel times and $O-C$ residuals for each station in the Western profile A.

| | Station | | Model I | | | Model II | |
|---|---|---|---|---|---|---|---|
| | | $T_0$ (sec) | | $T_c$ (sec) | $T_0-T_c$ (sec) | $T_c$ (sec) | $T_0-T_c$ (sec) |
| W | 1 Ôno | 7.10 | (L) | $P_1$ 7.09 | −0.01 | $P_1$ 7.16 | −0.06 |
| | 2 Nakai | 10.70 | | $P_{21}$ 10.71* | −0.01 | $P_2$ 10.70* | 0.00 |
| | 3 Utuo | 13.04 | | 〃 13.06 | −0.02 | 〃 13.09 | −0.05 |
| | 4 Mikata | 19.03 | | 〃 18.82 | 0.21 | 〃 18.93 | 0.10 |
| | 5 Ôi | 23.53 | | $P_{22}$ 23.52 | 0.01 | 〃 23.63* | −0.10 |
| | 6 Yatuai | 27.26 | (L) | $P_3$ 27.19* | 0.07 | $P_3$ 27.05 | 0.21 |
| | 7 Yasiro | 28.06 | | $P_{22}$ 28.03* | 0.03 | 〃 28.01 | 0.05 |
| | 8 Hukutiyama | 29.65 | | $P_3$ 29.82* | −0.17 | 〃 29.70 | −0.05 |
| | 9 Aogaki | 32.34 | | 〃 32.24 | 0.10 | 〃 32.19 | 0.15 |
| | 10 Ikuno | 35.07 | | 〃 35.11 | −0.04 | 〃 35.08 | −0.01 |
| | 11 Kawakami | 35.91 | | 〃 36.05* | −0.14 | 〃 35.96* | −0.05 |
| | 12 Yamazaki | 39.07 | | 〃 39.05 | 0.02 | 〃 39.03 | 0.04 |
| | 13 Kamigōri | 41.71 | | 〃 41.71 | 0.00 | 〃 41.72 | −0.01 |
| | 14 Yanahara | 44.26 | | 〃 44.25 | 0.01 | 〃 44.26 | 0.00 |
| | 15 Yakage | 49.6 ? | | 〃 51.23 | | | |

2. Remarks on the Bouguer anomaly of gravity

For reference sake, the Bouguer anomaly of gravity[6] along the present two profiles is added to Figs. 8 (a) and 9 (a). Comparing the crustal structure derived as Model I with the distribution of the anomaly,

Table 4. Calculated travel times and $O-C$ residuals for each station in the Western profile B.

| Station | $T_0$ (sec) | Model I $T_c$ (sec) | Model I $T_0-T_c$ (sec) | Model II $T_c$ (sec) | Model II $T_0-T_c$ (sec) |
|---|---|---|---|---|---|
| W 16 Arabuti | 2.09 | $P_1$ 2.08 | 0.01 | $P_1$ 2.10 | −0.01 |
| 17 Itosiro | 3.73 | 〃 3.73 | 0.00 | 〃 3.76 | −0.03 |
| 18 Ôgawara | 8.74 | $P_{21}$ 8.83* | −0.09 | $P_2$ 8.74* | 0.00 |
| 19 Gihu | 13.12 | 〃 13.10 | 0.02 | $P_2'$ 13.05 | 0.07 |
| 20 Kinomoto | 14.08 | 〃 14.12 | −0.04 | 〃 14.04 | 0.04 |
| 21 Kaizu | 17.91 | 〃 18.47 | −0.56 | 〃 17.93* | −0.02 |
| 23 Kitoge | 19.47 | 〃 19.40 | 0.07 | 〃 18.90 | 0.57 |
| 24 Imazu | 20.2 | $P_{22}$ 20.44 | −0.2 | 〃 20.03 | 0.2 |
| 25 Sirahige | 21.57 | 〃 21.55 | 0.02 | 〃 21.27 | 0.30 |
| 26 Takasima | 22.00 | 〃 22.05 | −0.05 | 〃 21.82 | 0.18 |
| 27 Kido | 23.95 | (L) $P_{21}$ 23.89 | 0.06 | 〃 23.51 | 0.44 |
| 28 Wani | 23.9 | $P_{22}$ 23.77 | 0.1 | 〃 23.75 | 0.2 |
| 29 Bessyo | 25.25 | 〃 25.32 | −0.07 | 〃 25.24 | 0.01 |
| 30 Kyôto | 27.20 | 〃 27.15 | 0.05 | 〃 27.13 | 0.07 |
| 31 Sikibigahara | 28.40 | 〃 28.39 | 0.01 | $P_3$ 28.29 | 0.11 |
| 32 Kameoka | 29.66 | $P_3$ 26.79* | −0.13 | 〃 29.76 | −0.10 |
| 33 Taki | 30.26 | 〃 30.16* | 0.10 | 〃 30.16 | 0.10 |
| 34 Abuyama | 30.69 | 〃 30.82* | −0.13 | 〃 30.57 | 0.12 |
| 36 Ôharano | 32.73 | 〃 32.72 | 0.01 | 〃 32.73 | 0.00 |
| 37 Rokkô | 36.05 | (L) $P_{22}'$ 36.11 | −0.06 | (L) $P_2$ 36.39 | −0.34 |
| 38 Tainohata | 37.10 | $P_3$ 37.11 | −0.01 | $P_3$ 37.11 | −0.01 |
| 39 Sizuki | 44.60 | (L) $P_{22}'$ 44.57 | 0.03 | (L) $P_2$ 44.65 | −0.05 |
| 40 Suhara | 43.9 ? | $P_3$ 42.96 | | $P_3$ 42.96 | |
| 41 Kitaama | 43.20 | $P_{32}$ 43.20 | 0.00 | $P_3'$ 43.16 | 0.04 |

outcrops of the 2nd layer at Nakai, Ôgawara, Ôi—Hukutiyama and Kameoka—Abuyama seem to correspond to a small negative anomaly near these areas, and a thickening of the 1st layer near Mikata and Kitoge to the maximum negative anomaly in the northern part of Lake Biwa. Moreover, a shallow boundary between the 1st and 2nd layers beneath

6) *loc. cit.*, 5), Part 2, 5 (1954).

Kamigōri, and that between the 2nd and 3rd layers below Kitaama are suggestive of a positive anomaly near those regions, respectively.

In other words, it can safely be said that the derived structure corresponds qualitatively to distribution of the Bouguer anomaly.

## 5. Concluding Remarks

From an analysis of the observed results of seismic waves from the Miboro Explosions, two probable models of crustal structure as shown in Figs. 5, 8 and 9 were derived for the Eastern and Western profiles, respectively.

Final results are as follows.

In the Eastern profile, Model I, the first and second layers indicate a downward warping. The deepest portion of the former occurs near Matusiro and that of the latter in the neighbourhood of the Tyûbu mountain region. Their deepest values are about 9 km and 38 km, respectively. This is a remarkable feature in Model I. This may be as expected hitherto from an isostatic hypothesis.

In Model II of the same profile the mean depth of the second discontinuity is estimated to be about 36 km.

In the Western profiles, Model I, thicknening of the first layer is found to occur in the northern part of Lake Biwa. The boundary surface between the second and third layers descends westwards, but seems to ascend toward Awazi Island. Its deepest value is nearly 36 km.

In Model II of the profiles the mean depth of the said boundary is 27–29 km.

Comparing the results in the two Western profiles, the first layer is thought to taper northwards (toward the Japan-Sea coast) from southern parts of the mentioned regions.

On the whole, no striking conflict exists between the structres over the said three profiles, on view of Model I.

The discontinuity surface between the second and third strata becomes deeper westwards from the Kwantô District with its deepest value in the Tyûbu mountain region, and in turn becomes shallower toward Miboro. This deepens again toward the Kinki District, but seems to be shallower beneath Awazi Island.

It may safely be said that the derived structure corresponds, at least qualitatively, to the Bouguer anomaly of gravity and to the struc-

ture deduced from spectrum of the anomaly[7].

The interface between the second and third strata may be regarded as the Mohorovičić discontinuity. There may be left, however, some doubt in respect to the adopted velocity of 7.70 km/sec being a little smaller for that in the mantle surface.

In order to gain a more precise knowledge of the deeper structure of the crust, it will be necessary in future to observe seismic waves at a longer distance.

**Acknowledgement**

Finally, we wish to express our heartfelt thanks to the other members of the Research Group for their kind advice. Our thanks are also due to Mrs. T. Huzita for her assistance in preparing this paper.

---

## 10. 御母衣爆破地震動観測による日本中部の地殻構造
## 第2部 地殻構造について

京都大学防災研究所 三雲 健
京都大学理学部地球物理学教室 大塚道男
気象庁 宇津徳治
東京大学理学部地球物理学教室 寺島敦
東京大学地震研究所 岡田惇

御母衣爆破地震動の観測資料を解析した結果，東方および西方の二つの測線に対して，第5,8,9図に示されるようなそれぞれ二つの地殻構造の model が得られた．

各観測点で記録された P 波初動の走時曲線はそれぞれ次のようなみかけ速度を示す．

Model I
- 東方測線 : 5.55, 5.86, 6.33, 7.91 km/sec
- 西方測線A : 5.55, 5.92, 6.32, 7.52 〃
- 西方測線B : 5.55, 5.81, 6.16, 7.45 〃

Model II
- 東方測線 : 5.5, 6.0, 7.9 〃
- 西方測線A, B : 5.5, 6.0, 7.5 〃

Model I においては，関東地方ですでに得られた結果を考慮して，これらの資料から 5.55, 6.00 および 7.70 km/sec の速度を持つた3層より成る構造が考えられた．

第1層は中部地方および琵琶湖北部で厚くなつており，約 9 km の厚さと推定される．また西方の二つの測線の構造を比較すると，これは南側より北側（日本海側）へ向つて薄くなつていると思われる．第2-3層境界面（恐らく Mohorovičić discontinuity と考えられる）は関東地方より西方へ向つて深くなり，中部山岳地方で約 38 km の深さを持ち，さらに西方へかけてはいつたん浅くなる．御母衣附近で数 28 km である．これは近畿地方へ向つてまた深くなるが，淡路島方面では浅いと考えられる．最深の値は約 36 km である．

Model II の立場に立てば，第2-3層境界面の平均の深さは，中部地方で約 36 km，近畿地方で 27-29 km である．しかしながらこの model においては東西両測線の構造に若干の矛盾を生ずる．

7) T. TOMODA, *Journ. Geod. Soc. Japan*, **6** (1960), 47-55.